Is the corrolate macrocycle innocent or noninnocent? Magnetic susceptibility, Mössbauer, 1H NMR, and DFT investigations of chloro- and phenyliron corrolates.

ARTICLE *in* JOURNAL OF THE AMERICAN CHEMICAL SOCIETY · JULY 2002

Impact Factor: 12.11 · Source: PubMed

J|A|C|S
ARTICLES
Published on Web 05/16/2002

Is the Corrolate Macrocycle Innocent or Noninnocent? Magnetic Susceptibility, Mössbauer, ^{1}H NMR, and DFT Investigations of Chloro- and Phenyliron Corrolates

Olga Zakharieva,[§] Volker Schünemann,[§] Michael Gerdan,[§] Silvia Licoccia,[†] Sheng Cai,[‡] F. Ann Walker,*[,‡] and Alfred X. Trautwein*[,§]

Contribution from the Institut für Physik, Medizinische Universität zu Lübeck, Ratzeburger Allee 160, 23538 Lübeck, Germany, Dipartimento di Scienze e Tecnologie Chimiche, Universitá di Roma Tor Vergata, Via della Ricerca Scientifica, 00133 Rome, Italy, and Department of Chemistry, University of Arizona, Tucson, Arizona 85721-0041

Received December 13, 2001

Abstract: In an attempt to determine the electron configuration of (anion)iron corrolates, i.e., whether they are S = 1 Fe(IV)-corrolate(3^-) or $S = {}^3/_2$ Fe(III)-corrolate($2^{-\bullet}$), with antiferromagnetic coupling between the iron and macrocycle electrons to yield overall $S = 1$, two axial ligand complexes of an iron octaalkylcorrolate have been studied by temperature-dependent magnetic susceptibility, magnetic Mössbauer, and ^{1}H NMR spectroscopy, and the results have been compared to those determined on the basis of spin-unrestricted DFT calculations. Magnetic susceptibility measurements indicate the presence of a noninnocent macrocycle (corrolate ($2^{-\bullet}$)) for the chloroiron corrolate, with strong antiferromagnetic coupling to the $S = {}^3/_2$ Fe(III) center, while those for the phenyliron corrolate are not conclusive as to the electron configuration. Temperature- and field-dependent Mössbauer spectroscopic investigations of these two complexes yielded spectra that could be simulated with either electron configuration, except that the isomer shift of the phenyl−iron complex is −0.10 mm/s while that of the chloroiron complex is +0.21 mm/s, suggesting that the iron in the former is Fe(IV) while in the latter it is Fe(III). ^{1}H NMR spectroscopic studies of both axial ligand complexes show large negative spin density at the *meso* carbons, with those of the chloroiron complex (Cai, S.; Walker, F. A.; Licoccia, S. *Inorg. Chem.* **2000**, *39*, 3466) being roughly four times larger than those of the phenyliron complex. The temperature dependence of the proton chemical shifts of the phenyliron complex is strictly linear. DFT calculations are consistent with the chloroiron complex being formulated as $S_1 = {}^3/_2$ Fe(III)-corrolate ($2^{-\bullet}$) $S_2 = {}^1/_2$, with negative spin density at all nitrogens and *meso* carbons, and a net spin density of −0.79 on the corrolate ring and positive spin density (+0.17) on the chloride ion and +2.58 on the iron. In contrast, the phenyliron complex is best formulated as $S = 1$ Fe(IV)-corrolate (3^-), but again with negative spin density at all nitrogens and *meso* carbons of the macrocycle, yet with the net spin density on the corrolate ring being virtually zero; the phenyl carbanion carbon has relatively large negative spin density of −0.15 and the iron +2.05. On the basis of all of the results, we conclude that in *both* the chloroiron and phenyliron complexes the corrolate ring is noninnocent, in the chloroiron complex to a much larger extent than in the phenyliron complex.

Introduction

Corroles are 18-electron aromatic macrocycles related to porphyrins, except that they have a direct link between two pyrrole rings and, when fully deprotonated, are trianionic ligands. They have unique properties such as the capability of maintaining a planar ring conformation, the possibility of stabilizing high oxidation states for coordinated metal ions,[1] and/or the possibility of stabilizing a one-electron oxidized macrocycle.[2] Recently, we reported NMR and EPR spectroscopic studies of two chloroiron corrolates, chloroiron octamethylcorrolate, [FeCl(OMCorr)], and chloroiron 7,13-dimethylhexaethylcorrolate, [FeCl(7,13-Me_2Et_6Corr)],[2] shown in Chart 1, their

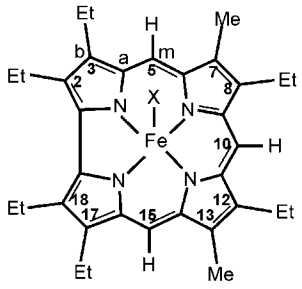

[FeX(7,13-Me_2Et_6Corr)]

X = Cl, Ph

a = α-carbon types

b = β-carbon types

m = *meso*-carbon types

* Corresponding author. E-mail: awalker@u.arizona.edu.
§ Medizinische Universität zu Lübeck.
† Universitá di Roma Tor Vergata.
‡ University of Arizona.

(1) Licoccia, S.; Paolesse, R. *Struct. Bonding* **1995**, *84*, 71.
(2) Cai, S.; Walker, F. A.; Licoccia, S. *Inorg. Chem.* **2000**, *39*, 3466.

10.1021/ja012701h CCC: $22.00

mono- and bisimidazole[2] and biscyanide[3] complexes, and the autoreduced cyanoiron(III) 7,13-dimethylhexaethylcorrolate anion, [FeCN(7,13-Me_2Et_6Corr)]$^-$.[3] More recently, we have also reported NMR studies of four chloroiron *meso*-triphenylcorrolates and the perchloratoiron analogue of one of them.[4] In all of the cases of the chloroiron corrolates,[2,4] the NMR spectra were interpreted as indicating that the metal oxidation and spin state were Fe(III), $S = {}^3/_2$, bound to a corrolate($2^{-\bullet}$) π-cation radical. The distinguishing features that led to this interpretation were the large positive *meso*-H chemical shifts of the β-pyrrole octaalkylcorrolates[2] and the large alternating-sign *meso*-phenyl-H shifts of the triphenylcorrolates,[4] both of which indicated large negative spin density on the corrolate ligand.

In contrast to the conclusions reached from NMR spectroscopic studies,[2,4] earlier investigations of chloroiron octaethylcorrolate, [FeCl(Et_8Corr)] or [FeCl(OECorr)], by Vogel and coworkers,[5] including Mössbauer spectroscopic measurements, suggested that an alternate electron configuration, Fe(IV)Cl bound to (OECorr)$^{3-}$, was the case for this complex. This alternate electron configuration was also assumed in a later electrochemical study of [FeCl(OECorr)], [FePh(OECorr)], and the 1-electron-reduced monopyridine complex, [Fe(Py)(OECorr], where the first two complexes were assumed to be Fe(IV)[6] while the 1-electron-reduced pyridine complex was interpreted as being $S = {}^3/_2$ Fe(III).[5,6] However, the Mössbauer parameters for $S = {}^3/_2$ Fe(III) and $S = 1$ Fe(IV) are in some cases very similar, and it was suggested[2] that for this reason, a more thorough magnetic Mössbauer spectroscopic study should be carried out in order to evaluate whether this technique could in fact be used to determine the oxidation and spin states of iron macrocycles for these two particular cases.

On the basis of the ^{1}H NMR[2,4] and Mössbauer[5] spectroscopic data for several chloroiron corrolates and the claims that chloroiron tri(pentafluorophenyl)corrolate has an Fe(IV) electron configuration,[7,8] Ghosh has recently reported DFT calculations that support the $S = {}^3/_2$ Fe(III) corrolate($2^{-\bullet}$) electron configuration,[9,10] and has hosted a series of papers in *JBIC* on high-valent metalloporphyrins and possible valence tautomerism to create macrocycle π-cation radicals,[10−16] in which it has been suggested that the corrolate ligand is noninnocent with respect to its electron configuration.[10]

This paper describes a detailed experimental investigation of two iron octaalkylcorrolates: [FeCl(7,13-Me_2Et_6Corr)] and [FePh(7,13-Me_2Et_6Corr)}, where Ph = $C_6H_5^-$ (see Chart 1). Magnetic susceptibility measurements over a wide temperature range, low-temperature magnetic Mössbauer, and variable-temperature ^{1}H NMR spectroscopic studies have been carried out on these two complexes. Density functional theory (DFT) calculations on the free-base octamethylcorrole (H_3OMCorr) and three iron complexes, chloro- and phenyliron octaethylcorrolate and chloroiron triphenylcorrolate, have also been carried out. The results show that the corrolate ligand is indeed noninnocent, and that magnetic susceptibility and magnetic Mössbauer spectroscopic measurements can, under certain circumstances, differentiate between $S = {}^3/_2$ Fe(III) corrolate($2^{-\bullet}$) and $S = 1$ Fe(IV) corrolate(3^-), while ^{1}H NMR data show clearly the noninnocence of the corrolate ligand in *both* complexes, but alone cannot evaluate the degree of noninnocence of each, and hence the overall bulk electron configuration. DFT calculations both corroborate the interpretation of the NMR data in terms of noninnocence of the corrolate ligand in both complexes, and are extremely helpful in understanding the effects of axial ligands and corrolate substituents on the electron configuration of the metal and spin density distribution in the corrolate ring.

Experimental Section

Synthesis. Chloroiron 7,13-dimethylhexaethylcorrolate, [FeCl(7,13-Me_2Et_6Corr)],[2] and phenyliron 7,13-dimethylhexaethylcorrolate, [FePh-(7,13-Me_2Et_6Corr)] (Ph = C_6H_5),[5] were synthesized as reported previously. ^{57}Fe powder (AMT Sales, Israel) was utilized to prepare highly enriched (95%) samples for Mössbauer spectroscopy according to general procedures published previously.[17]

Magnetic Susceptibility Measurements. Susceptibility measurements were performed in the temperature range 2−300 K in an applied field of 5 T using a SQUID magnetometer (MPMS, Quantum Design). The amount of material used for the measurements was 11.1 mg for [FeCl(7,13-Me_2Et_6Corr)] and 11.2 mg for [FePh[7,13-Me_2 Et_6Corr)]. The experimentally determined susceptibilities were corrected for the sample-holder signal and the diamagnetic contribution by using Pascal's constants.[18] The experimental data have been analyzed by a least-squares fit procedure with a full-matrix diagonalization, using the spin-Hamiltonian approach which includes, for spin-coupled systems, an isotropic Heisenberg−Dirac−Van Vleck (HDVV) exchange term $H = J\mathbf{S_1}\cdot\mathbf{S_2}$.[19]

Mössbauer Spectroscopic Measurements. Mössbauer spectra were recorded with a conventional spectrometer in the constant-acceleration mode. Isomer shifts, δ, are given relative to α-Fe at room temperature. The spectra obtained at 20 mT were measured in a He bath cryostat (Oxford MD 306) equipped with a pair of permanent magnets. For the high-field spectra, a cryostat equipped with a superconducting magnet was used (Oxford Instruments Spectromag 4000). Magnetically split spectra of paramagnetic samples were simulated in the spin-Hamilton approximation,[19] otherwise spectra were analyzed by least-squares fits using Lorentzian line shapes. The isomer shift and quadrupole splitting of [FeCl(TPCorr)] have been reported previously.[4]

NMR Spectroscopy. The NMR spectra of [FeCl(7,13-Me_2Et_6Corr)] as a function of temperature have been published previously.[2] NMR samples of [FePh(7,13-Me_2Et_6Corr)] were prepared in CD_2Cl_2 and were investigated on a Varian Unity-300 over the temperature range 30 to

(3) Cai, S.; Licoccia, S.; Walker, F. A. *Inorg. Chem.* **2001**, *40*, 5795.
(4) Cai, S.; Licoccia, S.; Paolesse, R.; Nardis, S.; Bulach, V.; Zimmer, B.; Shokhireva, T. Kh.; Walker, F. A. *Inorg. Chim. Acta*, **2002**, in press.
(5) Vogel, E.; Will, S.; Schulze Tilling, A.; Neumann, L.; Lex, J.; Bill, E.; Trautwein, A. X.; Wieghardt, K. *Angew. Chem., Int. Ed. Engl.* **1994**, *33*, 731.
(6) Van Caemelbecke, E.; Will, S.; Autret, M.; Adamian, V. A.; Lex, J.; Gisselbrecht, J.-P.; Gross, M.; Vogel, E.; Kadish, K. M. *Inorg. Chem.* **1996**, *35*, 184.
(7) Simkhovic, L.; Galili, N.; Saltsman, I.; Goldberg, I.; Gross, Z. *Inorg. Chem.* **2000**, *39*, 2704.
(8) Simkhovich, L.; Mahammed, A.; Goldberg, I.; Gross, Z. *Chem. Eur. J.* **2001**, *7*, 1041.
(9) Steene, E.; Wondimagegn, T.; Ghosh, A. *J. Phys. Chem. B* **2001**, *105*, 11406−11413.
(10) Ghosh, A.; Steene, E. *JBIC* **2001**, *6*, 739.
(11) Ghosh, A. *JBIC* **2001**, *6*, 726.
(12) Scheidt, W. R. *JBIC* **2001**, *6*, 727.
(13) Gross, Z. *JBIC* **2001**, *6*, 733.
(14) Renner, M. W.; Fajer, J. *JBIC* **2001**, *6*, 823.
(15) Weiss, R.; Bulach, V.; Gold, A.; Terner, J.; Trautwein, A. X. *JBIC* **2001**, *6*, 831.
(16) Watanabe, Y. *JBIC* **2001**, *6*, 846.
(17) Walker, F. A.; Huynh, B. H.; Scheidt, W. R.; Osvath, S. R. *J. Am. Chem. Soc.* **1986**, *108*, 5288.
(18) Kahn, O. *Molecular Magnetism*; VCH Publishers, Inc.: New York, 1993; p 3.
(19) Butzlaff, Ch.; Trautwein, A. X.; Winkler, H. In *Methods of Enzymology*; Vol. 227, Metallobiochemistry Part D: Physical and Spectroscopic Methods for Probing Metal Ion Environments in Metalloproteins; Riordan, J. F., Vallee, B. L., Eds.; Academic Press: San Diego, CA, 1993; p 412.
(20) Schünemann, V.; Winkler, H. *Rep. Prog. Phys.* **2000**, *63*, 263.
(21) Frish; et al. *Gaussian 98*, Revision A.5; Gaussian, Inc.: Pittsburgh, PA, 1998.

−80 °C. *J*-coupled resonances were assigned on the basis of COSY spectra (not shown). The assignments agreed with those reported previously for the closely related octaethylcorrolate.[5]

Computational Method

The DFT calculations were performed with the B3LYP method in Gaussian 98.[21] As basis set the all-electron basis[22−24] 6-3116 G was used for the first- and second-row elements and the all-electron basis optimized by Wachters[25] and Hay[26] for the transition-metal center. The MO wave functions were analyzed with the Molden program[27] in order to obtain electron density contour plots. The coordinate system was chosen such that the *x*-axis bisects the N−Fe−N angle and the $C_\alpha-C_\alpha$ bond of the macrocycle, while the *z*-axis is along the Fe−Cl(Ph) bond.

The structural data used for H_3OMCorr (Supporting Information, Figure S1a) are based on the structure of 8,12-diethyl-2,3,7,13,17,18 hexamethylcorrole.[27] To have symmetrical substituents, the two ethyl groups were replaced by methyl in the calculations. The structural data used for chloroiron octaethylcorrolate, [FeCl(OECorr)] (Supporting Information, Figure S1b), and phenyliron octaethylcorrolate, [FePh(OECorr)] (Supporting Information, Figure S1c), were taken from Vogel et al.[5] The axial ligands cause significant out-of-plane positions of the metal, i.e. 0.42[5] and 0.27[5] Å, respectively. Also, the iron−axial ligand bond distances are very different, i.e. 2.26 Å (Fe−Cl)[5] and 1.98 Å ($Fe-C_{phenyl}$).[5] The phenyl is fixed in a particular orientation with respect to its projection in the corrolate plane. It lies in a plane perpendicular to the corrolate plane, with the dihedral angle between the axial ligand plane and the closest Fe−N vector being nearly eclipsed.[5] For comparison, calculations on a chloroiron triphenylcorrolate, [FeCl(TPCorr)], were performed; its structural data are based on the structure of chloroiron tri(pentafluorophenyl)corrolate;[7] however, for the present calculations the F atoms were replaced by H atoms. The overall structure thus derived for [FeCl(TPCorr)] is very similar to that of [FeCl(OECorr)] in terms of macrocycle and axial ligand metrics.

Results and Discussion

Magnetic Susceptibility Measurements. The objective of analyzing the measured temperature dependence of the effective magnetic moment (μ_{eff}) of [FeCl(7,13-Me_2Et_6Corr)] and [FePh(7,13-Me_2Et_6Corr)] is to investigate (i) whether these two complexes feature "true" high-valent Fe(IV) $S = 1$ centers or (ii) whether instead the corrole ring is oxidized, i.e. is noninnocent. In this latter case the complexes would be $S_1 = {}^3/_2$ Fe(III), $S_2 = {}^1/_2$ corrolate ($2^{-\bullet}$) π-cation radical species, where the macrocycle radical electron is antiferromagnetically coupled to the metal electrons to give an overall $S = 1$ complex.

Case (i): For Fe(IV) $S = 1$ centers with zero-field splitting of $D < 40$ cm^{-1}, as observed in iron porphyrinates,[29] the magnetic moment of the complex above ~70 K is temperature independent and reaches the value ~2.9 μ_B. This is only achieved by appropriately correcting the experimental data for temperature-independent paramagnetism (TIP). The necessary TIP parameters for fitting the temperature-dependent susceptibility data for [FeCl(7,13-Me_2Et_6Corr)] and [FePh(7,13-Me_2Et_6Corr)] are 549 × 10^{-6} and 756 × 10^{-6} cm^3 mol^{-1}, respectively; these values are of the same order of magnitude as those estimated on the basis of the coupling between a magnetic ground state (with energy E_0) and a thermally nonpopulated excited state (with energy E_1).[30] Energy differences of the order of 10^4 cm^{-1}, which are not unusual for Fe(IV) $S = 1$,[29] yield TIP values of ~400 × 10^{-6} cm^3 mol^{-1}. The parameters obtained in the two-parameter fits of μ_{eff} (T) (Figure 1a,b) are $D = 36(2)$ cm^{-1}, $g = 1.92(2)$ for [FeCl(7,13-Me_2Et_6Corr)] and $D = 20(2)$ cm^{-1}, $g = 2.06(1)$ for [FePh(7,13-Me_2Et_6Corr)]. The $g_\perp$-factors of cytochrome P450 and HRP compound II analogues are certainly >2.0;[29] therefore the parameter set obtained for [FeCl(7,13-Me_2Et_6Corr)] indicates that the Fe(IV) $S = 1$ electronic configuration does not apply for the Cl-ligated corrolate. The $g_\parallel$-factors are actually smaller than, but very close to the value 2.00;[28] therefore we have recalculated the temperature dependence of the effective magnetic moment μ_{eff} of [FePh(7,13-Me_2Et_6Corr)] with $D = 20$ cm^{-1}, $g_\perp = 2.06$, and $g_\parallel = 2$ and found practically the same $\mu_{eff}(T)$ pattern as for the parameters $D = 20$ cm^{-1}, $g_\perp = g_\parallel = 2.06$. Thus, the parameter set obtained for [FePh(7,13-Me_2Et_6Corr)] is compatible with Fe(IV) $S = 1$ for the phenyliron corrolate.

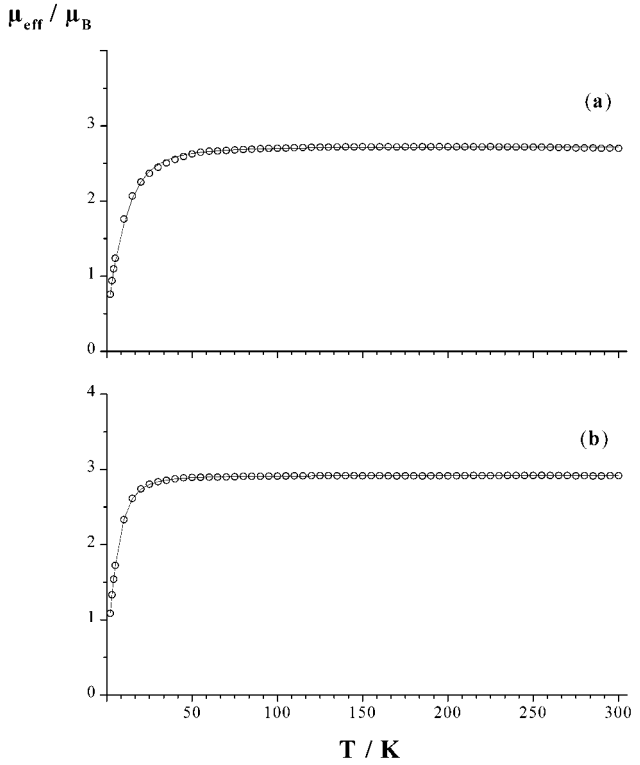

Figure 1. Temperature dependence of the effective magnetic moment μ_{eff} of (a) [FeCl(7,13-Me_2Et_6Corr)] and (b) [FePh(7,13-Me_2Et_6Corr)] obtained in a field of $B = 5$ T and corrected for diamagnetic contributions with use of Pascal's constants and for TIP = 550 × 10^{-6} cm^3 mol^{-1}. The solid lines are fits (based on the spin-Hamiltonian approach) assuming an Fe(IV) $S = 1$ center. The obtained-fit parameters are the following: (a) $D =$ 36 cm^{-1}, $g = 1.92$ for [FeCl(7,13-Me_2Et_6Corr)] and (b) $D = 20$ cm^{-1}, $g =$ 2.06 for [FePh(7,13-Me_2Et_6Corr)].

Case (ii): For antiferromagnetically exchange-coupled Fe(III) $S_1 = {}^3/_2$ corrolate π-cation radical $S_2 = {}^1/_2$ species, nonzero temperature dependence of $\mu_{eff}(T)$ above ~70 K is expected; i.e. the smaller the exchange-coupling constant J in $H = J\mathbf{S_1}\cdot\mathbf{S_2}$ the more μ_{eff} will increase with increasing temperature. The

(22) Hehre, W. J.; Radom, L.; Schleyer, P. v. R.; Pople, J. A. *Ab Initio Molecular Orbital Theory*; John Wiley & Sons: New York, 1986.
(23) Krishnan, R.; Binkley, J. S.; Seeger, R.; Pople, J. A. *J. Chem. Phys.* **1980**, *72*, 650.
(24) Krishnan, R.; Frisch, M. J.; Pople, J. A. *J. Chem. Phys.* **1980**, *72*, 4244.
(25) Wachters, A. J. H. *J. Chem. Phys.* **1970**, *52*, 1033.
(26) Hay, P. J. *J. Chem. Phys.* **1977**, *66*, 4377.
(27) Schaftenaar, G.; Noordik, J. H. *J. Comput.-Aided Mol. Design* **2000**, *14*, 123.
(28) Harrison, H. R.; Hodder, O. J. R.; Hodgkin, D. C. *J. Chem. Soc. (B)* **1971**, 640.
(29) Paulsen, H.; Müther, M.; Grodzicki, M.; Trautwein, A. X.; Bill, E. *Bull. Soc. Chim. Fr.* **1996**, *133*, 703.
(30) Reference 17, pp 7 and 8.

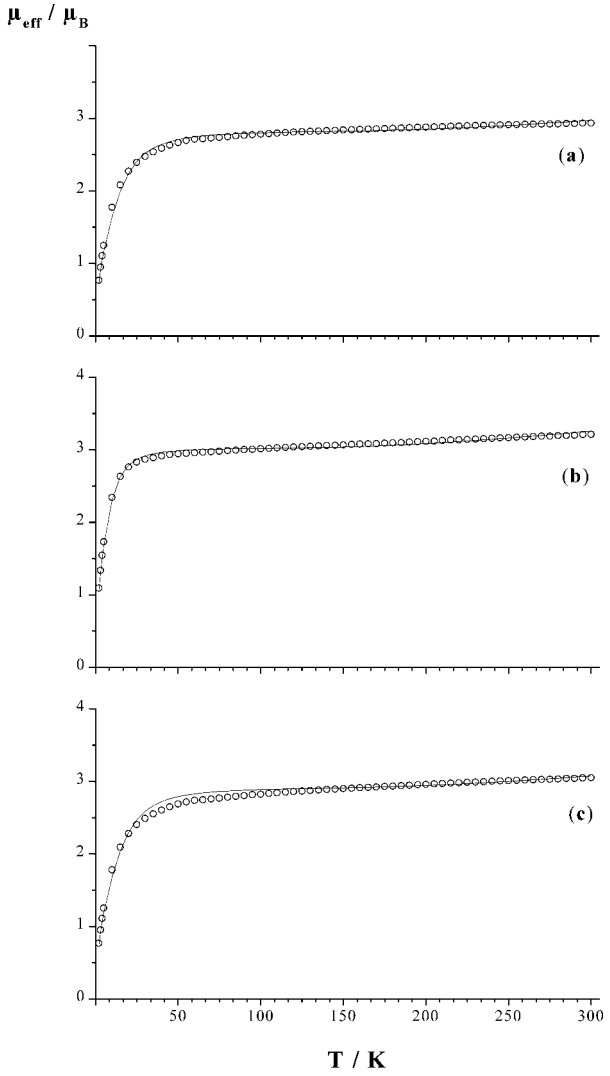

Figure 2. Temperature dependence of the effective magnetic moment μ_{eff} of (a, c) [FeCl(7,13-Me_2Et_6Corr)] and (b) [FePh(7,13-Me_2Et_6Corr)] obtained in a field of $B = 5$ T and corrected for diamagnetic contributions only, i.e. TIP = 0. The solid lines are fits (based on the spin-Hamiltonian approach) assuming antiferromagnetically exchange-coupled Fe(III) $S_1 = {}^3/_2$ corrolate π-cation radical ($S_2 = {}^1/_2$) species. The obtained parameters are the following: (a) $J = 350$ cm^{-1}, $D = 28$ cm^{-1}, $g = 2.00$ for [FeCl(7,13-Me_2-Et_6Corr)], (b) $J = 300$ cm^{-1}, $D = 15$ cm^{-1}, $g = 2.11$ for [FePh(7,13-Me_2-Et_6Corr)], and (c) $J = 343$ cm^{-1}, $D = 28$ cm^{-1} (fixed), $g = 2.05$ (fixed) for [FeCl(7,13-Me_2Et_6Corr)].

maximum increase of μ_{eff} with increasing temperature is achieved by not correcting the experimental μ_{eff} data for TIP. Thus, the situation with TIP = 0 provides an estimate for the lower limit of J in the three-parameter fits of $\mu_{eff}(T)$. The results obtained are (Figure 2 a,b) $J = 350(30)$ cm^{-1}, $D = 28(3)$ cm^{-1}, $g = 2.00(2)$ for [FeCl(7,13-Me_2Et_6Corr)] and $J = 300(30)$ cm^{-1}, $D = 15(2)$ cm^{-1}, $g = 2.11(2)$ for [FePh(7,13-Me_2Et_6Corr)]. To test the individual influence of one of the three parameters upon the simulated temperature variation of μ_{eff}, several one-parameter fits with fixed values for the other two parameters were performed, thus providing an estimate of the uncertainties of the three parameters. These estimates have been added in brackets to the values of J, D, and g given above. An example for the chloride complex, with fixed values for D (=28 cm^{-1}) and g (=2.05), yielding $J = 343$ cm^{-1}, is illustrated in Figure 2c.

In summary, we conclude that the magnetic susceptibility study of [FeCl(7,13-Me_2Et_6Corr)] indicates the presence of a noninnocent macrocycle in the chloride-ligated corrolate, while the results obtained for [FePh(7,13-Me_2Et_6C)] are not conclusive with respect to whether the macrocycle is innocent or noninnocent in the phenyl-ligated corrolate.

Mössbauer Spectroscopy. Temperature- and field-dependent Mössbauer studies of [FeCl(7,13-Me_2Et_6Corr)] and [FePh(7,13-Me_2Et_6Corr)] were performed to test the results obtained from the magnetic susceptibility investigation. Of specific interest in this respect were the obtained estimates of the exchange-coupling constant J. The coupling between Fe(III) $S_1 = {}^3/_2$ and the π-cation radical $S_2 = {}^1/_2$ was reported to be strongly antiferromagnetic in the case of the chloride-ligated corrolates, as evidenced by the very large positive NMR shifts of the *meso*-H resonances.[2] Strong antiferromagnetic coupling in the chloride-ligated complex [FeCl(7,13-Me_2Et_6Corr)], as derived from analyzing the temperature dependence of μ_{eff} (vide supra), is in agreement with this report; therefore J values of $\sim$300 cm^{-1} should be consistent with the Mössbauer data of [FeCl(7,13-Me_2Et_6Corr)]. However, in analogy to the imidazole-ligated corrolates, which have no or weak ferromagnetic coupling between metal and macrocycle electrons,[2] it could be anticipated that the phenyl-ligated corrolate [FePh(7,13-Me_2-Et_6Corr)] might exhibit weaker coupling. Mössbauer spectroscopy is an appropriate tool for distinguishing cases in which J is of the same order of magnitude as or smaller than D from the strong-coupling case[31] by simulating the magnetic hyperfine pattern of the Mössbauer spectra, as had been shown for cytochrome P450 and peroxidase compound I analogues.[29]

Figure 3 shows field-dependent Mössbauer spectra of [FeCl-(7,13-Me_2Et_6Corr)] taken at 4.2 K. The spectrum obtained in a field of 20 mT exhibits a doublet with isomer shift $\delta = 0.21$ mm/s and quadrupole splitting $\Delta E_Q = 3.03$ mm/s, very similar to the values reported previously for [FeCl(OECorr)] at 77 K ($\delta = 0.19$ mm/s, $\Delta E_Q = 2.99$ mm/s).[5,32] The value of the isomer shift is higher than typically observed for Fe(IV) $S = 1$[33−36] and represents more likely Fe(III) $S = {}^3/_2$.[37−40] A similar isomer shift (0.19 mm/s) and large quadrupole splitting $\Delta E_Q = 2.93$ mm/s have been reported for the triphenylcorrolate analogue, [FeCl(TPCorr)] at 77 K in zero applied field.[4] For the [FeCl-(7,13-Me_2Et_6Corr)] complex, the magnetically induced hyperfine

(31) The weak and strong coupling cases also can be distinguished by different temperature dependences of μ_{eff} provided the magnetic susceptibility is not obscured by magnetic artifacts. Such iron-containing artifacts would individually become visible in the Mössbauer spectra.
(32) Although the 1-electron-reduced complex, [Fe(Py)(OECorr)]$^-$, which, on the basis of magnetic moment (3.80 μ_B) was interpreted to be $S = {}^3/_2$ Fe(III), has a negative isomer shift ($\delta = -0.09$ mm/s, $\Delta E_Q = 3.88$ mm/s).[5]
(33) Shirane, G.; Cox, D. E.; Ruby, S. C. *Phys. Rev.* **1962**, *125*, 1158.
(34) Boso, B.; Lang, B.; McMurry, T. J.; Groves, J. T. *J. Chem. Phys.* **1983**, *79*, 1122.
(35) Jüstel, Th.; Müller, M.; Weyhermüller, Th.; Kressl, C.; Bill, E.; Hildebrandt, P.; Lengen, M.; Grodzicki, M.; Trautwein, A. X.; Nuber, B.; Wieghardt, K. *Chem. Eur. J.* **1999**, *5*, 793.
(36) Collins, T. J.; Fox, B. G.; Hu, Z. G.; Kostka, K. L.; Münck, E.; Rickard, C. E. F.; Wright, L. J. *J. Am. Chem. Soc.* **1992**, *114*, 8724.
(37) Kennedy, B. J.; Murray, K. S.; Zwack, P. R.; Homborg, H.; Kalz, W. *Inorg. Chem.* **1986**, 25, 2539.
(38) Fitzgerald, J. P.; Haggerty, B. S.; Rheingold, A. L.; May, L.; Brewer, G. A. *Inorg. Chem.* **1992**, *31*, 2006.
(39) Kostka, K. L.; Fox, B. G.; Hendrich, M. P.; Collins, T. J.; Rickard, C. E. F.; Wright, L. J.; Münck, E. *J. Am. Chem. Soc.* **1993**, *115*, 6746.
(40) Keutel, H.; Käpplinger, I.; Jäger, E.-G.; Grodzicki, M.; Schünemann, V.; Trautwein, A. X. *Inorg. Chem.* **1999**, *38*, 2320.
(41) This 1-electron-oxidized complex has been shown to have $\mu_{ef} = 1.73$ μ_b, and was suggested by the authors to contain Fe(IV) antiferromagnetically coupled to a corrolate(2$^{-\bullet}$) radical.[6] The 1-electron reduced complex, [FePh(OECorr)]$^-$, has a rhombic EPR spectrum with $g = 2.51, 2.19, 1.73$, and was interpreted to contain $S = {}^1/_2$ Fe(III).[6]

Table 1. Mössbauer Parameters of [FeCl(7,13-Me_2Et_6Corr)] Obtained from the Simulations Shown in Figure 3[a]

S_1	**g**[b]	*E*/*D*	D[b] (cm^{-1})	δ (mm/s)	ΔE_Q (mm/s)	α_v[c] (deg)	β_v[c] (deg)	γ_v[c] (deg)	Γ (mm/s)	η	**A**/$g_N\mu_N$ (T)	α_A[d] (deg)	β_A[d] (deg)	γ_A[d] (deg)
3/2	2.0	0	28	0.21	+3.02	−130(20)	15(5)	−80(20)	0.40	0.3(2)	−18(4)	0(15)	−30(5)	−95(20)
	2.0										5.4(1.7)			
	2.0										−18(4)			

[a] Note that the total spin is $S = 1$, because an antiferromagnetic coupling of $S_1 = 3/2$ with $S_2 = 1/2$ ($J = 350$ cm^{-1}) has been included in the analysis. [b] The **g** tensor, the zero-field splitting D, and the exchange-coupling constant J (=350 cm^{-1}) have been taken from the analysis of the susceptibility data. [c] Euler angles that describe the rotation from the principal axes of **g** to the axes of the electric field gradient tensor. [d] Euler angles that describe the rotation from the principal axes of **g** to the axes of the **A** tensor.

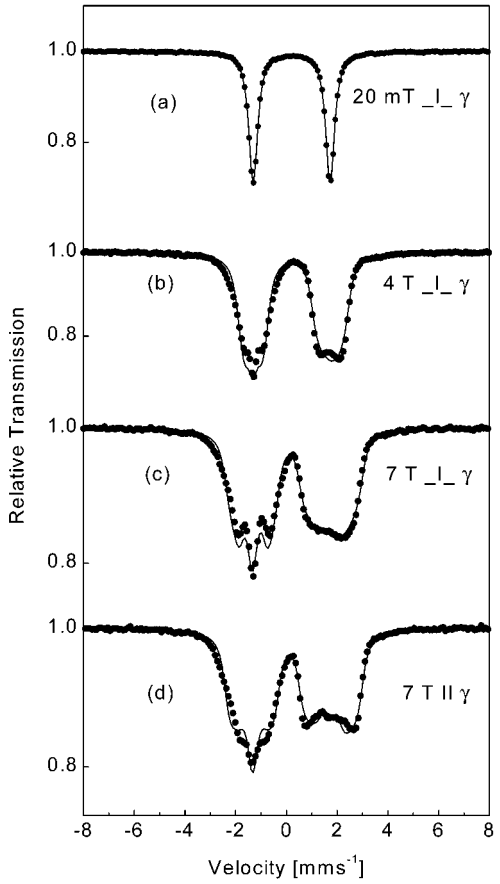

Figure 3. Field-dependent Mössbauer spectra of [FeCl(7,13-Me_2Et_6Corr)] obtained at 4.2 K and in applied fields as indicated. The solid lines are spin-Hamiltonian simulations assuming a spin-coupled system with $S_1 = 3/2$ on the iron center and $S_2 = 1/2$ on the macrocycle. The simulations have been performed with a coupling constant $J = 350$ cm^{-1} as obtained from the susceptibility data. The parameters of the ferric $S = 3/2$ site are listed in Table 1.

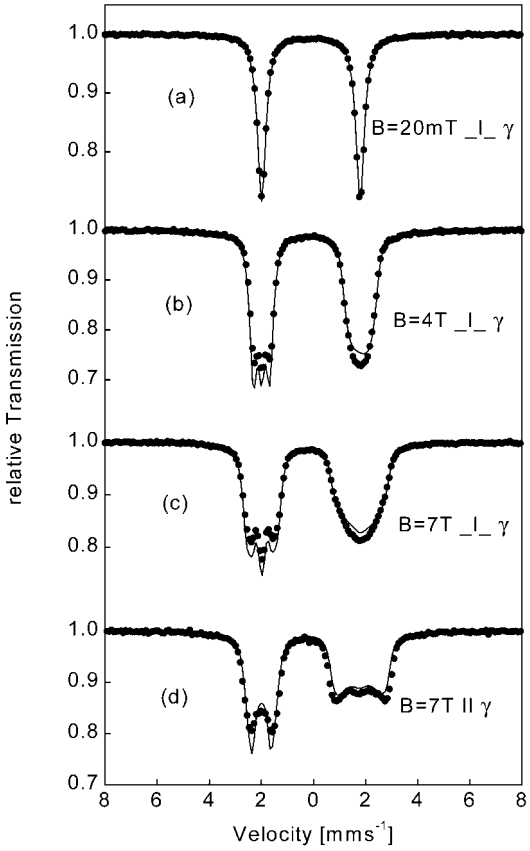

Figure 4. Field-dependent Mössbauer spectra of [FePh(7,13-Me_2Et_6Corr)] obtained at 4.2 K and in applied fields as indicated. The solid lines are spin-Hamiltonian simulations assuming an $S = 1$ iron center with the parameters listed in Table 2.

Table 2. Mössbauer Parameters of [FePh(7,13-Me_2Et_6Corr)] Obtained from the Simulations Shown in Figure 4

S	**g**[a]	*E*/*D*	D[a] (cm^{-1})	δ (mm/s)	ΔE_Q (mm/s)	Γ (mm/s)	η	**A**/$g_N\mu_N$ (T)
1	2.06	0	20	−0.10	+3.74	0.30	0	−16.8 (2.0)
	2.06							−16.8 (2.0)
	2.00							−10.0 (5.0)

[a] The g-tensor and the zero-field splitting D have been taken from the analysis of the susceptibility data.

splitting therefore has been simulated by a spin-Hamiltonian formalism that includes strong antiferromagnetic coupling of $S_1 = 3/2$ on the iron and $S_2 = 1/2$ on the macrocycle. The exchange-coupling constant of $J = 350$ cm^{-1} as well as the zero-field splitting $D = 28$ cm^{-1} and the g-factors ($g = 2.00$) have been taken from the analysis of the susceptibility data. The isomer shift η and the quadrupole splitting ΔE_Q result from the fit of the quadrupole doublet recorded in 20 mT at 4.2 K (Figure 3a), and the positive sign of the main component of electric field tensor (efg) and the small asymmetry parameter of the efg ($\eta = 0.3 \pm 0.2$) from the 4 T Mössbauer spectrum recorded at 100 K (see Supporting Information, Figure S2). Thus the rhombicity parameter E/D, the components of the hyperfine coupling tensor **A**, and the Euler angles remain as free parameters. The successful simulation of four experimental spectra with the parameter set summarized in Table 1 is shown in Figure 3.

Figure 4 shows field-dependent Mössbauer spectra of [FePh-(7,13-Me_2Et_6Corr)] taken at 4.2 K. In a field of 20 mT a quadrupole doublet with $\delta = -0.10$ mm/s and $\Delta E_Q = 3.78$ mm/s is observed, very similar to the values reported previously for [FePh(OECorr)] at 77 K ($\delta = -0.11$ mm/s, $\Delta E_Q = 3.72$ mm/s),[5,6] and also very similar to those observed for its

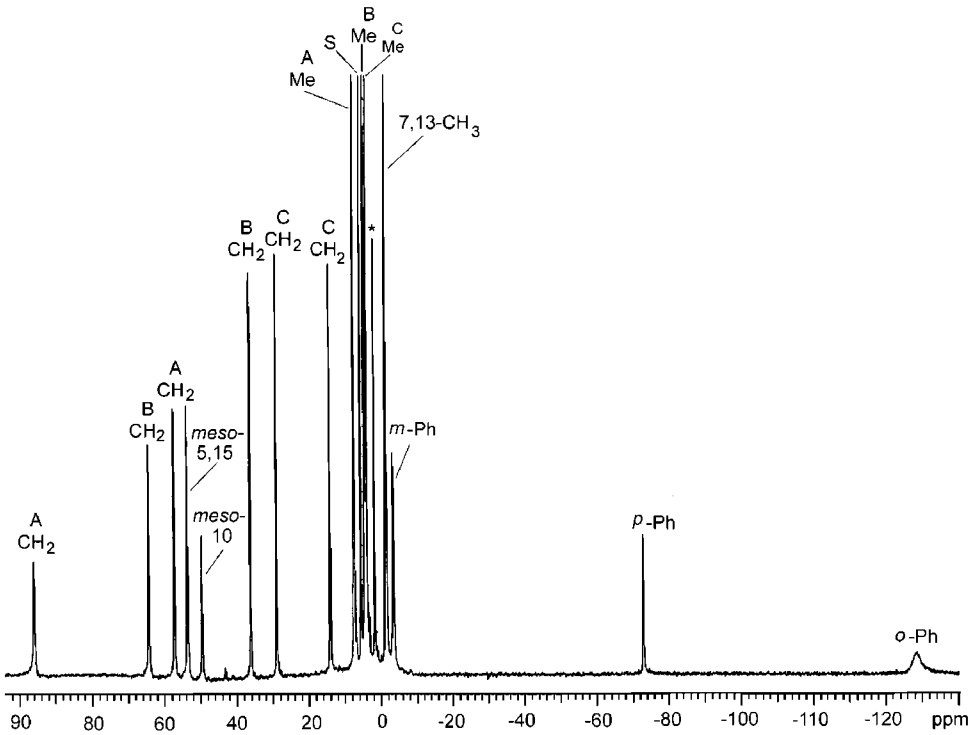

Figure 5. 1D ^{1}H NMR spectrum of [FePh(7,13-Me_2Et_6Corr)] in CD_2Cl_2 at 30 °C. *J*-coupled ethyl groups are shown by the letters A, B, and C.

1-electron-oxidation product, [FePh(OECorr)ClO_4], at 120 K ($\Delta = -0.10$ mm/s, $\Delta E_Q = 3.66$ mm/s).[6,41] The negative value of the isomer shift is indicative of an iron center in the formal valence state of Fe(IV).[31−34] The application of large external fields induces magnetic hyperfine splitting, which has been simulated by the spin-Hamiltonian formalism with the parameters given in Table 2. These parameters represent an Fe(IV) $S = 1$ complex and include the same D (=20 cm^{-1}) and g values ($g_\perp = 2.06$, $g_\parallel = 2.00$) as obtained from the analysis of the susceptibility data discussed above. The positive sign of the main component of the efg and the zero asymmetry parameter of the efg are confirmed by measurements taken at 150 K in a field of 4 T (Supporting Information, Figure S3).

In summary, we note that the isomer shift of [FeCl(7,13-Me_2Et_6Corr)] (and [FeCl(TPCorr)][4]) falls in the range of Fe(III) $S = {}^3/_2$ complexes while that of [FePh(7,13-Me_2Et_6Corr)] lies closer to the values characteristic of Fe(IV) $S = 1$ species,[32−36] and is very similar to that of the 1-electron-oxidized [FePh(OECorr)ClO_4], which has been formulated as an antiferromagnetically coupled $S_1 = 1$ Fe(IV), $S_2 = {}^1/_2$ corrolate(2$^{-\bullet}$) electron configuration.[6,41] Therefore we have only shown simulations which correspond to a spin-coupled $S_1 = {}^3/_2$ Fe(III), $S_2 = {}^1/_2$ corrolate π-cation radical species in Figure 3 and to an Fe(IV) $S = 1$ corrolate in Figure 4. However, with the exception of the isomer shift, it is also possible to simulate the spectra in Figure 3 with the parameters of an Fe(IV) $S = 1$ species and the spectra of Figure 4 correspondingly with the parameters of a strongly coupled Fe(III) $S_1 = {}^3/_2$ π-cation radical $S_2 = {}^1/_2$ species (not shown). Thus, the magnetic Mössbauer patterns are not sensitive for distinguishing $S = 1$ Fe(IV) and $S_1 = {}^3/_2$ Fe(III) $S_2 = {}^1/_2$ π-cation radical species. This is only true if spin coupling in the Fe(III) species is very strong; if it were weak, the Fe(IV) and Fe(III) species would significantly differ in their magnetic Mössbauer patterns. Simulations with small values for J (of the order of magnitude of D; not shown), however, do not reproduce the hyperfine patterns of the measured Mössbauer spectra, for either [FeCl(7,13-Me_2Et_6Corr)] or [FePh(7,13-Me_2Et_6Corr)].

^{1}H NMR Spectroscopic Investigations. The ^{1}H NMR spectra of [FeCl(7,13-Me_2Et_6Corr)] have been reported and their temperature dependence analyzed previously.[2] Therefore, we will first present the new results for [FePh(7,13-Me_2Et_6Corr)], and then compare and contrast these results to those of the chloride complex.

Figure 5 shows the 1D proton NMR spectrum of [FePh(7,13-Me_2Et_6Corr)] in CD_2Cl_2 at 30 °C, including the *m*-H, *p*-H, and *o*-H resonances of the phenyl group (identified via their COSY correlations in the case of the *m*- and *p*-H resonances (not shown) at −3.7 and −73.2 ppm, respectively); the *o*-H resonance, which relaxed too rapidly to produce COSY correlations, is found at −148 ppm. The *J*-coupled ethyl resonances (determined from COSY spectra, not shown) are marked A, B, and C; we have tentatively assigned them as 3,17- (A), 2,18- (C), and 8,12- (B), based upon the spin densities calculated from DFT methods (see below). This assignment is different from that based upon a comparison to Mn octaalkylcorrolates reported previously,[42] where methyl/ethyl substitution allowed complete assignment of all resonances. (In contrast, the tentative assignments of the ethyl resonances for [FeCl(7,13-Me_2Et_6Corr)],[2] based upon the calculated spin densities (see below), are consistent with those given previously,[2] which were based upon comparison to the Mn octaalkylcorrolates.[42]) Neither NOESY nor NOE difference spectra provided data that could be used to

(42) Licoccia, S.; Morgante, E.; Paolesse, R.; Polizo, F.; Senge, M. O.; Tondello, E.; Boschi, T. *Inorg. Chem.* **1997**, *36*, 1564.

(43) Walker, F. A. In *The Porphyrin Handbook*; Kadish, K. M., Smith, K. M., Guilard, R., Eds.; Academic Press: San Diego, CA, 2000; Chapter 36, Vol. 5, pp 81−183.

Table 3. ^{1}H Chemical Shifts of [FeCl(7,13-Me_2Et_6Corr)][a] and [FePh(7,13-Me_2Et_6Corr)][b] in CD_2Cl_2

[FeCl(7,13-Me_2Et_6Corr)],[a] 300 K		[FePh(7,13-Me_2Et_6Corr)],[b] 303 K				
chemical shift, ppm	isotropic shift,[c] ppm	chemical Shift, ppm	isotropic shift,[c] ppm	dipolar shift, ppm	contact shift, ppm	assignment
174	164.2 (−0.23)[e]	53.4	43.6	+9.7	33.9 (−0.04)[e]	5,15-*meso*-H
187	177.3 (−0.26)[e]	49.4	39.7	+9.7	30.0 (−0.04)[e]	10-*meso*-H
29.7, 17.3, *0.6*[d]	25.5, 13.1, *-1.3*[d] (+0.05)[e]	28.7, 13.9, *3.7*[d]	24.5, 9.7[d]	+3.8[d]	20.7, 5.9[d] (−0.01)[e]	2,18-CH_2-*CH_3*[f]
20.9, −5.2, *2.5*[d]	16.9, −9.2, *0.6*[d] (−0.04)[e]	95.7, 57.0, *7.1*[d]	91.7, 53.0[d]	+3.8[d]	87.9, 49.2[d] (+0.06)[e]	3,17-CH_2-*CH_3*[f]
18.0	14.2 (+0.02)[e]	−1.7	−5.5	+3.8[d] (−0.002)[e]	−9.3	7,13-CH_3
27.3, 4.1, *1.3*[d]	23.2, 0.0, *−0.6*[d] (−0.01)[e]	65.2, 35.9, *4.3*[d]	61.1, 48.9[d]	+3.8[d]	57.3, 44.1[d] (+0.02)[e]	8,12-CH_2-*CH_3*[f]
		−148	−144.6	−18.7	−125.9 (+0.047)[e]	*o*-Ph-H
		−3.7	−9.6	−10.2	+0.6 (−0.026)[e]	*m*-Ph-H
		−73.2	−79.5	−8.9	−70.6 (+0.032)[e]	*p*-Ph-H

[a] Data taken from ref 2. [b] This work. [c] Isotropic shift = observed chemical shift − diamagnetic shift. Diamagnetic shifts taken from ref 60 for ethyl and phenyl substituents, and from ref 61 for methyl substituents. For the phenyliron complex, the calculated dipolar shifts are given in parentheses. [d] Italicized numbers are for methyl protons of the ethyl groups. Isotropic shifts for these methyl protons were not calculated. [e] C_β spin density obtained from DFT calculations. [f] Tentative assignments based on the relative spin densities obtained from DFT calculations for both complexes.

aid in assignment of the ethyl groups of [FePh(7,13-Me_2Et_6-Corr)]. The chemical shifts of all resonances at 30 °C are listed in Table 3. The chemical shifts of the related complex, [FePh-(OECorr)], and the assignments of proton types, at ambient temperatures in $CDCl_3$, have been reported previously,[5] and are similar to those observed in Figure 5 and Table 3, except for the 7,13-methyl resonance of the present complex and the ethyl resonances from this ring position (which we can now assign by process of elimination as those at 6.4, −8.4 (CH_2), and 3.0 (CH_3) ppm) observed for [FePh(OECorr)].[5]

As shown in Figure 5, the 5,15- and 10-*meso* resonances are at 53.4 and 49.4 ppm, respectively, chemical shifts that are clearly not those expected for a simple Fe(IV) complex with one unpaired electron in each of the d_π orbitals, d_{xz}, and d_{yz}. Such an electron configuration would produce small negative chemical shifts for the *meso*-H resonances (due to the small spin density expected at the *meso* positions, resulting from spin delocalization from the metal d_π orbitals to the 3e*(π)*-related orbitals of the corrolate ring, which are expected to have very small spin density), probably more negative than those seen for the corresponding Fe(IV) porphyrinate complexes (3 to −3 ppm),[43] but not significantly more so. Instead, quite positive chemical shifts for these *meso* protons are observed. Before discussing the implications of these positive chemical shifts for the *meso*-H, however, the temperature dependence of all of the resonances of [FePh(7,13-Me_2Et_6Corr)] will be discussed.

In Figure S4 (Supporting Information) are shown the chemical shifts of the protons of [FePh(7,13-Me_2Et_6Corr)], plotted vs. 1/*T*. All resonances extrapolate to the diamagnetic region of the NMR spectrum, suggesting that the spin state of [FePh(7,13-Me_2Et_6Corr)] is pure, with no low-lying, thermally accessible excited states being available, and no detectable curvature resulting from a D/T^2 dipolar shift contribution to the observed chemical shift or isotropic shift, as is expected for this $S > {}^1/_2$ metal center with a nearly isotropic **g**-tensor.[44] For an $S = 1$ Fe(IV) center, this dipolar shift is given by[44]

$$\delta_{dip} = -\{2\mu_B{}^2(g_{||}{}^2 + {}^1/_2 g_\perp{}^2)D/27k^2T^2\}[(3\cos^2\theta - 1)/R^3],$$

where μ_B is the Bohr magneton, *k* is the Boltzmann constant, *T* is the absolute temperature, and the term within square brackets is the geometric factor that interrelates the position of each proton to the Cartesian and polar coordinate axes.[43,45] With $D = 20\ cm^{-1}$ as found in the magnetic susceptibility measurements discussed above, this expression yields estimated[46] dipolar shifts (including those for the phenyl group) at 303 K that range from 3.8 to 18.7 ppm in magnitude, as included in the dipolar shift column for this complex in Table 3. At the lowest temperature for which the ^{1}H NMR chemical shifts were measured, 193 K, the calculated dipolar shifts are about 2.5 times larger than those at 303 K, yet within experimental error, the phenyliron corrolate obeys the Curie law. It is possible, however, that a thermally accessible excited state[47] exists that effectively cancels the curvature expected[44] due to the D/T^2 dipolar term.

The calculated phenyl-H contact shifts are large and negative for the *o*- and *p*-H, but very small, yet slightly positive, for the *m*-H (Table 3). This alternating sign pattern of contact shifts is expected for π-spin delocalization[43,45] from iron to the phenyl ligand, except that the *m*-H contact shift is smaller in magnitude relative to the *o*- and *p*-H than usually observed (Table 3). DFT calculations to be discussed below yield alternating signs for the spin densities at the *o*-, *m*-, and *p*-carbons, with more similar magnitudes of the spin densities than indicated by the contact shifts presented in Table 3, consistent with π-spin delocalization (spin densities included in Table 3 in parentheses in the contact shift column).

The isotropic shifts of [FePh(7,13-Me_2Et_6Corr)] are compared to those of [FeCl(7,13-Me_2Et_6Corr)][2] in Table 3. As mentioned above, the assignment of the ethyl groups to the various corrolate ring positions is tentative. However, even if these ethyl group assignments were certain, their chemical shift values are not as indicative of the spin density distribution as are protons directly attached to the π system of the macrocycle, because of the

(44) Kurland, R. J.; McGarvey, B. R. *J. Magn. Reson.* **1970**, *2* 286.
(45) La Mar, G. N.; Walker, F. A. In *The Porphyrins;* Dolphin, D., Ed.; Academic Press: New York, 1979; Vol. IV; ppl 61−157.
(46) Geometric factors (for octaethylporphyrin and axial pyridine as a model of the phenyl ligand) were taken from Table 7 of ref 43, and the permittivity of free space, μ_0, was used for SI unit conversion.
(47) Shokhirev, N. V.; Walker, F. A. *J. Phys. Chem.* **1995**, *99*, 17795.

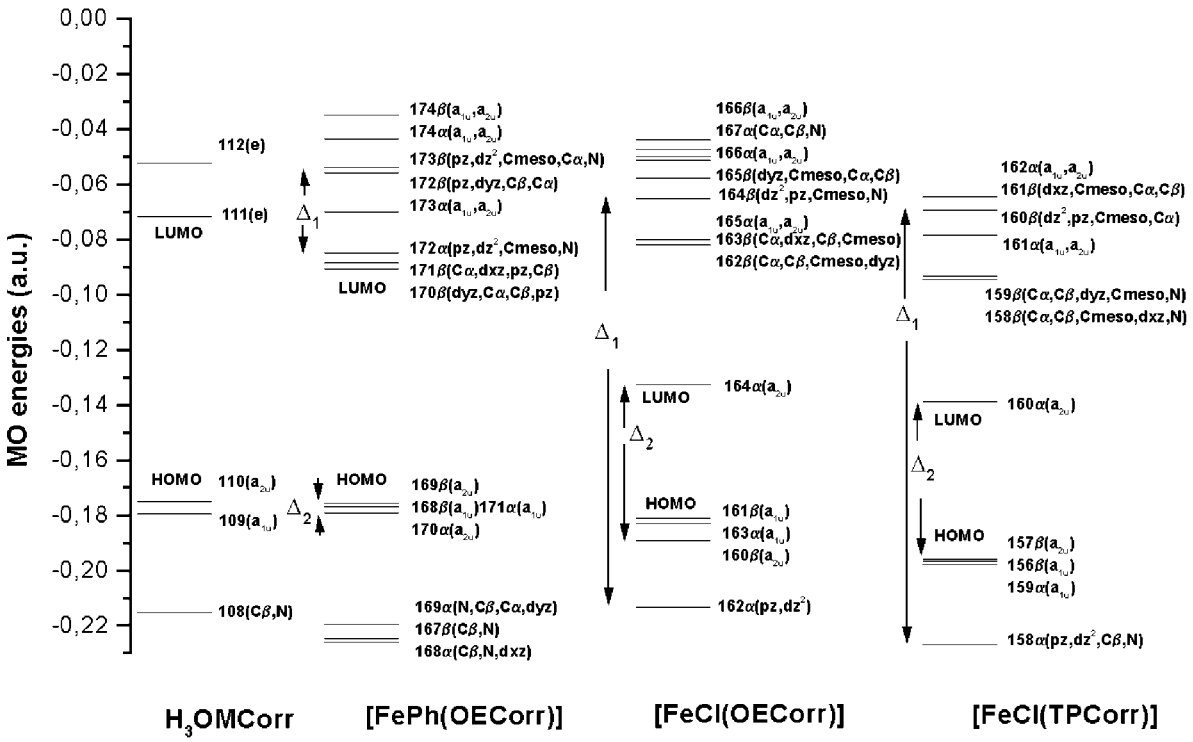

Figure 6. Calculated orbital energy diagram for H_3OMCorr, [FeCl(OECorr)], [FeCl(TPCorr)], and [FePh(OECorr)].

unknown average rotational conformations of the methylene protons.[43,45] Thus, we will first concentrate on the *meso*-H chemical shifts of the two compounds. Dipolar and contact shifts have not been calculated for the chloroiron complex because of the uncertainty as to the dipolar shifts if this is a $S_1 = {}^3/_2$, $S_2 = {}^1/_2$ antiferromagnetically coupled complex. For this case, at a maximum, the dipolar shifts could be a factor of 4.5 times[44] the ratio of the zero-field splitting constants (28/20, Tables 1 and 2) for the two complexes, or about 6.3 times larger for the $S = {}^3/_2$ metal than those listed in Table 3 for the $S = 1$ phenyliron complex. However, even with such large dipolar shifts, the *meso*-H isotropic shifts are still largely contact in origin.[48]

As has been discussed in detail elsewhere,[43,45] for cases in which positive spin density is delocalized from a metal into a ligand π system through either L → M or M → L π donation, for protons directly bound to a carbon that is part of the π system, negative contact shifts are expected theoretically, and observed experimentally.[49] Hence, the very large *positive* isotropic (and contact) shifts observed for the *meso*-H of [FeCl(7,13-Me_2Et_6Corr)] are a clear indication that *there is large negative spin density* at the *meso*-carbons of this complex. As pointed out previously,[2] this large *negative* spin density at the *meso*-carbons clearly identifies this complex as one in which there is an unpaired electron on the macrocyclic ring that is antiferromagnetically coupled to the unpaired electrons on the metal. This conclusion, that the electron configuration and spin state of [FeCl(7,13-Me_2Et_6Corr)] are $S = {}^3/_2$ Fe(III) bound to a corrolate($2^{-\bullet}$) π-cation radical,[2] is now corroborated by the magnetic susceptibility and magnetic Mössbauer spectroscopic data presented above. But in contrast to these results, for the other complex, [FePh(7,13-Me_2Et_6Corr)], the Mössbauer isomer shift was more consistent with an Fe(IV) corrolate(3^-) formulation. Nevertheless, the NMR data for the phenyliron complex show the *meso*-H resonances at 53.4 and 49.4 ppm, yielding contact shifts of 33.9 and 30.0 ppm for the 5,15- and 10-H (Table 3). Thus, we see that the observed positive sign for the phenyliron corrolate *meso*-H shifts, as for the chloroiron corrolate, is again indicative of negative spin density at the *meso*-carbons, yet the magnitudes are only a fraction (∼20−25%) of the negative spin densities for the chloroiron complex. The large negative spin densities at these *meso*-carbons is thus not compatible with the assignment of the corrolate ring of the phenyliron complex as a completely innocent (simple 3^-) anionic macrocycle, and cannot be accounted for quantitatively without carrying out theoretical calculations. Such calculations are discussed in the following section.

DFT Calculations. Density functional theory (DFT) constitutes a computationally expedient method that has been shown to successfully describe ground-state electronic properties of

(48) The likelihood that the dipolar shifts are not as large as this maximum estimate is supported by the fact that the average isotropic shift of the methylene protons tentatively assigned to the 3,17-ethyl groups (Table 3) is positive (+3.9 ppm), yet the calculated spin density is negative and almost as large in magnitude as that for the average isotropic shift of the methylene protons tentatively assigned to the 2,18-ethyl groups (+19.3 ppm),[49] and that the average isotropic shift of the methylene protons tentatively assigned to the 8,12-ethyl groups is large and positive (+11.6 ppm) even though the spin density calculated at that position is within experimental error of zero. These observations suggest that the dipolar shift of the methylene protons is of the order of +11.6 ppm, or about half the estimated maximum value. This would suggest that the average contact shift of the 2,18-methylene protons is about +7.7 ppm and that of the 3,17-methylene protons is about −7.7 ppm. However, this assumes that the average of the two methylene proton shifts in each case represents an isotropic proton distribution, which may not be the case.

(49) On the other hand, for protons attached to an alkyl carbon that is attached to a carbon that is part of a π system, positive spin density at the latter carbon produces a *positive* contact shift.[43,45]

(50) Salzmann, R.; McMahon, M. T.; Godbout, N.; Sanders, L. K.; Wojdelski, M.; Oldfield, E. *J. Am. Chem. Soc.* **1999**, *121*, 3818.
(51) Godbout, N.; Sanders, L. K.; Salzmann, R.; Havlin, R. H.; Wojdelski M.; Oldfield, E. *J. Am. Chem. Soc.* **1999**, *121*, 3829.
(52) Ghosh, A.; Wandimagegn, T.; Parusel, A. B. J. *J. Am. Chem. Soc.* **2000**, *122*, 5100.

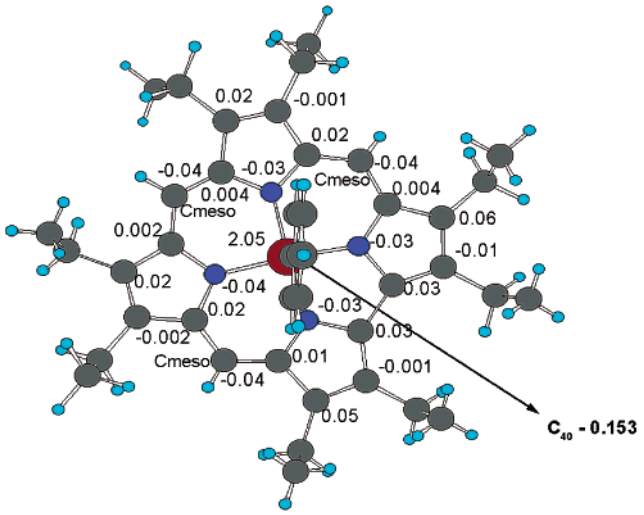

Figure 7. Calculated atomic spin-density distribution for [FePh(OECorr)].

transition metal porphyrinate systems.[50−52] In the present investigation we have explored the electronic structure of a corrole free base and three iron corrolates, starting with the metal-free system, octamethylcorrole (H_3OMCorr), and then introducing iron and different axial ligands (Cl^- and Ph^- ($C_6H_5^-$)), and equatorial substituents (octaethylcorrole and *meso*-triphenylcorrole).

Octamethylcorrole Free Base. The energy diagram derived from the DFT calculations for H_3OMCorr is shown in Figure 6. The two HOMOs (MO 109 and 110) are nearly degenerate and roughly correspond to the a_{1u} and a_{2u} orbitals of porphyrins; likewise, the two LUMOs, which are "e-like," are also of relatively similar energy. For H_3OMCorr these four frontier (closed-shell) orbitals are well-separated energetically from the rest of the orbital energy spectrum, but this is not the case for the metallocorrolates discussed below. The electron density contour plots of HOMO and HOMO-1 are shown in Figure S5a,b (Supporting Information). The "a_{2u}-like" HOMO exhibits significant C_{meso} and N, and the "a_{1u}-like" HOMO-1 C_α, C_β character (for C_α, C_β, C_{meso}, and N assignment, see Chart 1). The porphyrin-corrole analogy is limited because of the two different molecular symmetries, D_{4h} for porphyrin and C_2 for corrole macrocycles, ignoring the protons on the nitrogens, and is intended here mainly for the use of appropriate and convenient shorthand notations.

Metal-Substituted Corrolates. The metal-substituted corrolates [FeCl(OECorr)], [FeCl(TPCorr)], and [FePh(OECorr)] are paramagnetic, and require spin-unrestricted calculations. The obtained energy terms, other than for H_3OMCorr, are therefore represented by open-shell (α = spin up and β = spin down) orbitals (Figure 6). The orbitals at the HOMO/LUMO frontier are, in the metal-substituted corrolates, also crude analogues of the a_{1u} and a_{2u} porphyrinate orbitals for the HOMOs. The DFT calculations reveal, however, a striking difference in occupancy of these open-shell orbitals for the two chloroiron corrolates compared to the phenyliron corrolate and, thus, mirror the energetics of what, in analogy to porphyrinates, would be termed "metal- versus corrolate-centered oxidation".[52]

For [FePh(OECorr)] the "a_{1u}-like" α-spin (HOMO-2) and "a_{1u}-like" β-spin (HOMO-1) orbitals as well as the "a_{2u}-like" α-spin (HOMO-3) and "a_{2u}-like" β-spin (HOMO) orbitals are occupied and nearly degenerate energetically (Figure 6), indicating that the corrolate does not carry an overall spin in this case. Thus, the macrocycle is not oxidized to a π-cation radical, and could be said to be "innocent". However, in Figure 7 it becomes clear that although there is near-zero *net* spin density, the individual carbon and nitrogen atoms of the macrocycle carry either positive or negative spin density, with the signs alternating on most adjacent atoms. Specifically, all four nitrogens carry negative spin density (−0.03 to −0.04), and for comparison to the NMR data, we see that all three *meso*-carbons also carry negative spin density (−0.04), while the α-pyrrole carbons to which they are attached have smaller positive spin density (0.002−0.02). This pattern of alternating signs of the spin densities is reminiscent of that of an "odd-alternant hydrocarbon radical fragment",[53] and has been observed many times in NMR and EPR studies of such radicals. The spin at the C_β atoms also changes sign in an alternating fashion among the eight C_β positions. The accumulation of small negative spin densities on the N and C_{meso} atoms is due to small electron reorganization in the system via the a_{2u}-like corrolate orbitals MO 170α and 169β (Figure 6). However, as mentioned above, the *net* spin density on the corrolate ring of [FePh(7,13-Me_2Et_6Corr)] is vanishingly small (+0.01). Concomitant with this and in agreement with the "metal- versus corrolate-centered oxidation" alternative, the metal exhibits spin density of ca. +2, arising mainly from d_{xz} and d_{yz} contributions (Table 4), which is typical for Fe(IV) $S = 1$. The relatively small Fe d_{z^2} α-spin density of +0.27 is due to contributions from MOs with Fe d_{z^2} amplitude, which are located in the occupied region of the orbital energy diagram.

The phenyl axial ligand shows a *net* negative spin density of −0.08 on the entire phenyl moiety, or −0.15 at the carbanion center, C_{40} (Table 4); the *o*-, *m*-, and *p*-carbons are calculated to have spin densities of +0.047, −0.026, and +0.032, respectively. (Again, the pattern of alternating signs of the π spin densities is reminiscent of that of an odd-alternant hydrocarbon radical fragment,[51] if the metal is also included.) Comparison of these calculated spin densities to the NMR contact shifts is included in Table 3 and was mentioned above in the NMR section. The fact that the positive *m*-H contact shift of the phenyliron complex is much smaller in magnitude than would be suggested by the size of the calculated spin density and that for the phenyliron complex the smallest average methylene shift is opposite in sign to that predicted by the (very small) calculated spin density (Table 3) may suggest the limits in the ability of these DFT calculations to reproduce the experimental data for cases of small spin density. Nevertheless, the comparison between contact shifts and calculated spin densities is quite satisfying overall.

The situation is different for the two chloroiron corrolates. The DFT calculations reveal that the "a_{1u}-like" α-spin and "a_{1u}-like" β-spin-orbitals are nearly degenerate; they are represented by HOMO-1 and HOMO for [FeCl(OECorr)] and by HOMO-2 and HOMO-1 for [FeCl(TPCorr)] (Figure 6). However, the "a_{2u}" α-spin and "a_{2u}" β-spin-orbitals are clearly separated energetically, with the "a_{2u}" β-spin-orbital remaining occupied (HOMO-3 for [FeCl(OECorr)] and HOMO for [FeCl(TPCorr)]), while the "a_{2u}" α-spin-orbital is shifted into the unoccupied region of the orbital energy spectrum shown in Figure 6 (LUMO for both; i.e., 164α for [FeCl(OECorr)] (Supporting Information,

(53) Carrington, A.; McLachlan, A. D. *Introduction to Magnetic Resonance*; Harper: New York, 1967; pp 89−94.

Table 4. Calculated Total Spin Density on the Iron, on the Corrolate, and on the Axial Ligand and Distribution of the d Spin Density among the Fe 3d Orbitals

metal corrolate	iron	d_{z^2}	d_{xz}	d_{yz}	$d_{x^2-y^2}$	d_{xy}	corrolate	axial ligand
[FePh(OECorr)]	2.05	0.27	0.80	0.81	0.09	0.04	+0.01	−0.08 (−0.15)[a]
[FeCl(OECorr)]	2.58	0.68	0.86	0.86	0.05	0.13	−0.79	+0.17
[FeCl(TPCorr)]	2.58	0.67	0.86	0.82	0.05	0.13	−0.65	+0.18

[a] Spin density on the carbon atom directly ligated to iron.

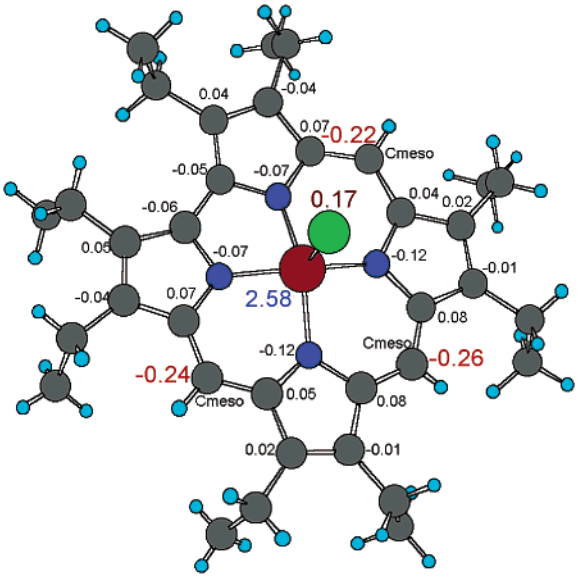

Figure 8. Calculated atomic spin-density distribution for [FeCl(OECorr)].

Figure S6) and 160α for [FeCl(TPCorr)] (not shown)). This scenario corresponds to the removal of an electron from an α-spin corrolate molecular orbital and indicates that the macrocycle is oxidized and noninnocent, with the unpaired spin density profile of a corrolate π-cation radical. This differs from the earlier assumed (by some workers) electron configuration, where the metal was assumed to have the +4 oxidation state and the corrolate ligand a simple −3 charge.[5,8,13] Figure 8 illustrates the gross atomic spin populations of this radical for [FeCl(OECorr)]. Those for [FeCl(TPCorr)] are shown in Figure S7 in the Supporting Information.

This corrolate radical exhibits relatively large negative spin density amplitudes (−0.07, −0.12) at the four nitrogens, and even larger at the C_{meso} positions (−0.22 to −0.26), or approximately $^1/_4$ of a negative-spin unpaired electron on each *meso*-carbon, consistent with the ^{1}H NMR results. The α-carbons adjacent to these *meso* positions carry smaller *positive* spin density in all cases; the spin densities on the β-pyrrole carbons alternate in sign as one traverses from the directly bound pyrrole rings to the other two, as they do for the phenyliron complex, and again the spin density distribution is reminiscent of that of an odd-alternant hydrocarbon.[53] Hence again, the corrolate ligand is noninnocent with respect to having both negative and positive spin density present on the macrocycle, yet in this case there is large *net* negative spin density on the macrocycle. Thus, the negative spin densities at the *meso* positions of the chloroiron corrolates are 5−6 times larger than those for the phenyliron corrolate, in relatively good agreement with the relative magnitudes of the ^{1}H isotropic (and derived contact) shifts of the *meso*-H of the two complexes presented in Table 3.

The net (integrated) atomic spin densities of this radical amount to about −0.79 and −0.65 (β-spin density) for the OECorr and TPCorr cases, respectively. The loss of one α-spin corrolate molecular orbital from the occupied region of the orbital energy spectrum is counterbalanced by the appearance of another α-spin-orbital in this region, i.e. an orbital with significant Cl p_z and Fe d_{z^2} contributions (HOMO-3 for [FeCl(OECorr)] (Figure 9) and for [FeCl(TPCorr)] (not shown)). The additional Fe d_{z^2} α-spin density contribution arising from this orbital causes an increase of iron α-spin density for the chloroiron corrolates as compared to that for the phenyliron corrolate (Table 4). In addition, the axial chloride ligand accumulates positive spin density; in other words, it supports additionally the process of electron transfer from corrolate to iron by creating α-spin density on the chloride ion. The pathway for this spin transfer is mainly via d_{z^2} (Figure 9).

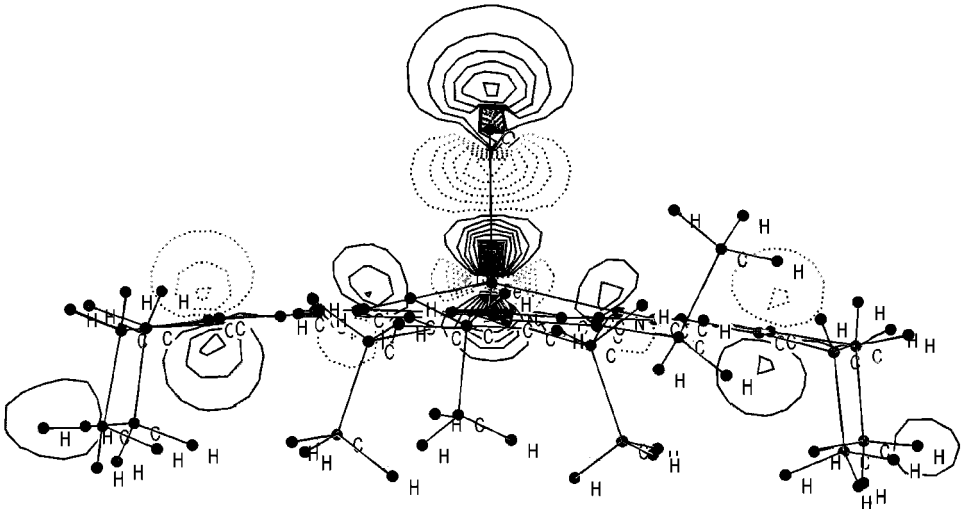

Figure 9. Calculated electron-density contour map of HOMO-3 (162α with Fe d_{z^2}, Cl p_z contributions) for [FeCl(OECorr)].

The main features of the electronic structure discussed so far are related to the energy separation Δ_2 of "a_{2u}" α-spin and "a_{2u}" β-spin-orbitals and with Δ_1 of "Cl p_z, Fe d_{z^2}" α-spin and "Cl p_z, Fe d_{z^2}" β-spin-orbitals (Figure 6). The center-of-mass of Δ_2 is about the same for the three metallocorrolates, while that of Δ_1 is much lower in energy for the chloroiron corrolates than for the phenyliron corrolate. Additionally, Δ_1 and Δ_2 are much larger for the former than for the latter. The net effect of these different energy separations and their concomitant orbital occupations are given below:

(1) In [FePh(OECorr)] the corrolate remains a simple 3^- ligand with practically zero *net* spin density on the macrocycle, yet is noninnocent, for it has negative spin density at all four nitrogens and all three *meso*-carbons, small positive spin density on the α-pyrrole carbons adjacent to these *meso*-carbons, and alternating signs of spin density on the β-pyrrole positions as one moves from the directly attached pyrrole rings to the other two symmetry-related pyrrole rings (the total $\alpha + \beta$ spin density on the corrole macrocycle, ignoring the sign, is in fact 0.534, nearly $^1/_2$ an electron, divided almost exactly equally between α and β spins); the axial phenyl-ligand donor atom C_{40} carries small negative spin density of -0.15, and the spin density of $+2.05$ on the iron corresponds to Fe(IV), $S = 1$.

(2) In [FeCl(OECorr)] and [FeCl(TPCorr)] the corrolate is one-electron oxidized and noninnocent, with *net* negative spin density of -0.7 to -0.8, and relatively large negative spin density at all *meso* carbons, smaller negative spin density at all nitrogens, smaller positive spin density on all pyrrole α-carbons to which the nitrogens and *meso*-carbons are attached, and alternating-sign spin density on the pyrrole β-carbons (the total $\alpha + \beta$ spin density, ignoring the sign, in this case is 1.83, or nearly 2 complete electrons, divided unequally between α and β spins); the axial chloride ligand carries a small positive spin density of $+0.17$, and the spin density of $+2.58$ on the iron approaches that of a ferric iron with intermediate spin; the overall electronic structure may be described, to a significant degree, as involving antiferromagnetic coupling between the Fe(III)-axial ligand unit and a corrolate π-cation radical. These results are in qualitative agreement with those reported recently for chloroiron corrolates;[9] the absolute spin densities are different (e.g. for iron $+2.00$[9] instead of $+2.58$ (this work)), presumably because the spin-unrestricted DFT calculations carried out by Ghosh et al. used the VWN local functional, with PW91 gradient corrections, and Slater-type valence triple-ζ plus polarization basis sets, while in the present study we have used the possibly somewhat better functionals of the B3LYP method together with optimized all-electron basis sets (see the Computational Method section).

In terms of bonding interactions that cause the chloride axial ligand to favor the Fe(III) π-cation radical electron configuration while the phenyl carbanion axial ligand favors the Fe(IV) electron configuration, we should recall the findings of the corresponding 1-electron-oxidized complexes of Fe(III) porphyrinates: It has been shown that if the axial ligand is a weaker π-donor and/or softer ligand such as chloride or bromide, then iron(III) porphyrinate π-cation radicals are formed, whereas a strong π-donor (in addition to its σ-donor interaction) such as a phenyl anion can help to stabilize Fe(IV).[15] The strong π-donation from the phenyl axial ligand has in some sense the effect of preventing electron donation from the corrolate ligand to iron. Thus the chloride axial ligand plays a substantial role in the electron transfer by favoring an intramolecular transfer process from corrolate to iron. On one hand, the chloride ligand encourages the process of corrolate spin transfer to iron by also accumulating positive spin density, while on the other hand the axial ligand shows an indirect influence on the spin density distribution, by causing geometrical changes (displacement of the iron out of the corrolate plane), and as a result changes in the interactions of the iron with the corrolate atoms occur. The insertion of substituents only on the *meso* positions enhances this process very slightly, as can be seen from the higher spin density at the chloride in the case of [FeCl(TPCorr)] as compared to [FeCl(OECorr)] ($+0.183$ vs $+0.166$, respectively). Otherwise, the two systems have very similar features and the same electron configuration for the metal center. This means that the main factor that determines the electron configuration in these corrolate complexes is the availability of a chloride axial ligand and not the substituents on the macrocycle, which are of similar electronic effects.[54]

Table 5. Calculated DFT Fe 3d Orbital Occupations

metal corrolate	d_{z^2}	d_{xz}	d_{yz}	$d_{x^2-y^2}$	d_{xy}	Σ 3d
[FePh(OECorr)]	1.03	1.05	1.09	1.57	0.87	5.61
[FeCl(OECorr)]	1.13	1.08	1.09	1.87	0.55	5.72
[FeCl(TPCorr)]	1.13	1.08	1.11	1.86	0.54	5.72

The main structural changes when going from the chloroiron to the phenyliron corrolates are the following:[5] (i) the Fe−N bond length decreases from 1.90 to 1.87 Å; (ii) the Fe−axial ligand bond length decreases from 2.26 to 1.98 Å; and (iii) the out-of-plane location of iron decreases from 0.42 to 0.27 Å. Removal of an electron from a corrolate molecular orbital to form a metallocorrolate π-cation radical complex leads to structural changes, or, conversely, structural changes enforce electronic structure changes which may lead to corrolate radical formation; both causal interpretations may illustrate the actual situation, as shown by the following examples:

(A) Decreasing the occupancy of the "a_{2u}" MO decreases the metal−nitrogen interaction because of the high amplitudes of this MO on the corrolate nitrogens. Such a trend has been reported previously for the Cu(III) corrolate, which was calculated to exhibit shorter metal−nitrogen bond distances compared to the Cu(II) corrolate radical valence tautomer.[52] At the same time, the Fe−N bond distances are shorter in the phenyliron corrolate than in the chloroiron corrolates. Or opposite to this line of interpretation: metal corrolate(3^-) complexes such as [FePh(OECorr)] provide stronger metal−nitrogen interaction, i.e. shorter metal−nitrogen bond distances, than corrolate π-cation radicals, as in [FeCl(OECorr)] and [FeCl(TPCorr)].

(B) In the presence of a strongly basic axial ligand, the corrolate macrocycle is reported to be fairly innocent, i.e. does not have radical character, with the unpaired spin density being entirely localized on the metal−axial ligand unit as shown for metal (Fe^{IV}, Mn^{IV})−oxo corrolates.[10] The phenyl carbanion in [FePh(OECorr)] is by far a more strongly basic axial ligand than Cl^- in [FeCl(OECorr)] and [FeCl(TPCorr)]; this effect is amplified by the short iron−carbon distance of 1.98 Å compared to the relatively long iron−chloride distance of 2.26 Å. In light

(54) For substituents with very different electronic effects, such as the *meso*-pentafluorophenyl substituents of [FeCl(TF_5PCorr)],[7,8] it is possible, though improbable,[4] that the electron configuration is different; our calculations do not address the electronic effects of this substituent.

Table 6. Calculated and Measured Mössbauer Parameters

	quadrupole splitting ΔE_Q(mm s^{-1})		asymmetr parameter η		electron density $\rho(0)$ (a_o^{-3})	isomer shift δ (mm s^{-1})	$\Delta\delta$ (mm s^{-1})	
metal corrolate	calcd	measd	calcd	measd	calcd[a]	measd[b]	calcd[d]	measd
[FePh(OECorr)]	+3.62	+3.78(3)	0.06	0.0(2)	11,617.71	−0.10		
[FeCl(OECorr)]	+3.02	+2.89(3)	0.02	0.3(1)	11,616.79	+0.21	0.26	0.30
[FeCl(TPCorr)]	+2.97	+2.93(3)[e]	0.11		11,616.83	+0.19[e]	0.25	0.29

[a] Values calculated with the atoms-in-molecules program AIM,[62] which uses the wave functions evaluated by the DFT program. [b] Values measured at 4.2 K relative to α-Fe at room temperature. [c] Values given relative to the isomer shift of [FePh(OECorr)]. [d] Values derived from $\Delta\delta = \alpha\Delta\rho(0)S_{cor}$, with $\alpha = -0.22$ mm s^{-1} a_o^3 and the relativistic correction factor $S_{cor} = 1.3$.[56] [e] Experimental data taken from ref 4.

of these arguments the corrolate ring is expected to be a 3$^-$ anion in [FePh(OECorr)], in agreement with our DFT calculations.

(C) Antiferromagnetic coupling of metal spin and corrolate radical spin involves metal (d_{z^2})−corrolate (a_{2u}) overlap, which is facilitated by the out-of-plane displacement of iron.[9,10] Because of the larger displacement of 0.42 Å for the chloroiron corrolates compared to 0.27 Å for the phenyliron corrolate, the antiferromagnetically coupled metallocorrolate radical state seems to be more likely for [FeCl(OECorr)] and [FeCl(TPCorr)] than for [FePh(OECorr)], also in agreement with our results.

(D) The larger iron−chloride bond distance (2.26 Å) as compared to the shorter iron−phenyl bond length (1.98 Å) results in reduced ligand p_z-iron d_{z^2} σ-antibonding interaction, with the result that the corresponding d_{z^2}-containing MOs are lower in energy for the chloroiron than for the phenyliron corrolate.

Spin Density Distribution versus Metal d-Orbital Occupancy. The DFT calculations provide distributions of spin density among the Fe 3d orbitals for the three metallocorrolates (Table 4) which approximately represent the following electronic configurations: (i) $(d_{x^2-y^2})^2(d_{xz})^1(d_{yz})^1$ for [FePh(OECorr)] and (ii) $(d_{x^2-y^2})^2(d_{xz})^1(d_{yz})^1(d_{z^2})^1$ for [FeCl(OECorr)] and [FeCl(TPCorr)]. Spin densities arise from the difference of α- and β-spin-orbital occupancies, and are the basis for the interpretation of magnetic properties (magnetic hyperfine interaction, magnetic susceptibility, NMR shifts, etc.). On the other hand, orbital occupancies arise from the sum of α- and β-spin-orbital contributions and are the basis for the interpretation of nonmagnetic properties such as the Mössbauer quadrupole splitting and isomer shift; they may, however, induce a different view of electron configurations compared to those derived from spin-density distributions. According to the results summarized in Table 5, the overall Fe 3d occupancy is close to $3d^{5.5}$, with considerable $3d_{xy}$ contribution for the three iron corrolates, which is different from what one expects for either the $(d_{x^2-y^2})^2(d_{xz})^1(d_{yz})^1$ or the $(d_{x^2-y^2})^2(d_{xz})^1(d_{yz})^1(d_{z^2})^1$ configuration. This manufactured discrepancy shows that whether it is justified to use, for qualitative interpretations, one electron configuration or another depends on the specific molecular property being investigated. The anisotropy of Fe 3d orbital occupations,

$$\Delta n(3d) = n(3d_{xy}) + n(3d_{x^2-y^2}) - n(d_{z^2}) - \frac{1}{2}[n(d_{xz}) + n(d_{yz})]$$

which is 0.34 for [FePh(OECorr)], 0.20 for [FeCl(OECorr)], and 0.17 for [FeCl(TPCorr)] (Table 5), describes qualitatively correctly the decrease of the corresponding quadrupole splittings from +3.62 mm s^{-1} to +3.02 and +2.97 mm s^{-1} (Table 6). However, the large positive ΔE_Q values are not well represented by the Δn(3d) from above. Quantitative agreement between calculated and measured quadrupole splittings (Table 6) in the present case is achieved in the DFT calculations by the refined 3d contributions, which arise from 15 (instead of 5) 3d basis orbitals. This refined description of the anisotropy of Fe 3d charge mirrors realistically the electric field gradient close to the iron nucleus. Therefore, the view that the iron in [FePh(OECorr)] is of Fe(IV) type and in [FeCl(OECorr/TPCorr)] is of Fe(III) type is not needed.

This is also true with respect to the isomer shift, though the value $\delta = -0.10$ mm s^{-1} measured for [FePh(OECorr)] is commonly used as an indication of the presence of a nonoxo-bound Fe(IV),[33−36] in particular when, simultaneously, the spin state of the metal is $S = 1$.[55] Since the overall Fe 3d occupancy for the three iron corrolates is practically equal and close to $3d^{5.5}$, as mentioned above, the reduction of isomer shift from ca. +0.20 mm s^{-1} for the chloroiron corrolates to −0.10 mm s^{-1} for the phenyliron corrolate cannot be explained by decreased potential shielding of iron core s orbitals when going from a $3d^5$ to a $3d^4$ configuration.[56] The only explanation for the significant difference of isomer shifts of 0.30 mm s^{-1}, therefore, is the difference of Fe 4s occupancy for the two cases. Inspection of the occupancy of the iron s basis orbitals indeed reveals that only the orbitals representing Fe 4s are involved in the increase of electron density at the iron nucleus, $\rho(0)$, by going from the chloroiron corrolates to the phenyliron corrolate. The calculated increase of 4s occupancy is 0.14, which together with $\rho_{4s}(0) \sim 7$ a_o^{-3} for the $3d^{5.5}4s$ configuration[56] amounts to a relativistic electron-density increase of $\Delta\rho(0) \sim 1$ a_o^{-3}. According to the relation $\Delta\delta = \alpha\cdot\Delta\rho(0)$ ($\alpha = -0.22$ mm s^{-1} a_o^3),[56] the corresponding calculated decrease of isomer shift is $\Delta\delta = -0.22$ mm s^{-1}. This estimate illustrates that the main contribution to the experimentally determined variation $\Delta\delta$ is due to the variation of Fe 4s occupancy and not due to an Fe(III)−Fe(IV) related change of $3d^n$ configuration.

Summary

In summary, we note that the DFT results consistently explain the differences of spin density-related, as well as charge density-related, molecular properties of the chloro- and phenyliron

(55) Trautwein, A. X.; Bill, E.; Bominaar, E. L.; Winkler, H. *Struct. Bonding* **1991**, *78*, 1.
(56) Reschke, R.; Trautwein, A. X.; Desclaux, J. P. *J. Phys. Chem. Solids* **1977**, *38*, 837.
(57) Buisson, G.; Deronzier, A.; Duee, E.; Gans, P.; Marchon, J.-C.; Regnard, J.-R. *J. Am. Chem. Soc.* **1982**, *104*, 6793.
(58) Phillippi, M. A.; Goff, H. M. *J. Am. Chem. Soc.* **1979**, *101*, 7641.
(59) Phillippi, M. A.; Shimomura, E. T.; Goff, H. M. *Inorg. Chem.* **1981**, *20*, 1322.
(60) Kadish, K. M.; Will, S.; Adamian, V. A.; Walther, B.; Erben, C.; Ou, Z.; Guo, N.; Vogel, E. *Inorg. Chem.* **1998**, *37*, 4573.
(61) Paolesse, R.; Licoccia, S.; Boschi, T. *Inorg. Chim. Acta* **1990**, *178*, 9.
(62) Biegler-König, F. *AIM 2000*, Version 1.0; University of Applied Science: Bielefeld, Germany 2000.

corrolates. From our findings, we conclude that the "metal- versus corrolate-centered oxidation" model applies only for the interpretation of magnetic properties, which are, nonetheless, very important.

We also note that the antiferromagnetic coupling between the $S_1 = {}^3/_2$ Fe(III) and $S_2 = {}^1/_2$ π-cation radical centers of the chloroiron corrolates results from symmetry-allowed overlap of the d_{z^2} orbital of the out-of-plane iron with the "a_{2u}-type" orbital of the corrolate ring, as pointed out previously by Ghosh and co-workers.[9] Such a pathway is not available to the six-coordinate iron(III) porphyrinate π-cation radicals such as the high-spin $S = {}^5/_2$ [Fe(OEP)($OClO_3$)$_2$] and admixed $S = {}^3/_2$, ${}^5/_2$ [Fe(TPP)($OClO_3$)$_2$] complexes, which are both ferromagnetically coupled,[12,57] because the metal is in the plane of the macrocycle. The direct five-coordinate Fe(III) porphyrinate π-cation radical analogue of the chloroiron corrolate of this study, [FeCl(TTP)]$^+$-SbF_6^-, exhibits alternating-sign ^{1}H NMR phenyl-H shifts that indicate that the unpaired electron on the macrocycle is antiferromagnetically coupled to the iron electrons.[57−59] The structure of the complex has been reported, and shows extreme saddling of the macrocycle,[57] which is another means of achieving antiferromagnetic coupling in $S > {}^1/_2$ iron(III) porphyrinates, in this case via coupling between the unpaired electron in the $d_{x^2-y^2}$ orbital of the $S = {}^5/_2$ Fe(III) porphyrinate and the a_{2u} porphyrin π orbital.[57] This means of achieving antiferromagnetic coupling may be more favorable for the porphyrinate, which is larger than the corrolate ring, and is thus able to saddle; the chloroiron octaalkyl corrolates are not saddled.[5,6] Furthermore, the smaller macrocycle hole of the corrolate ligand does not support the high-spin Fe(III) electron configuration that would make this type of macrocycle distortion and electron coupling possible.

In terms of the energies of the HOMOs of these three iron complexes, obtained from the DFT calculations reported herein (Figure 6), we note that those of the phenyl- and chloroiron complexes of OECorr are relatively similar, while the energy of the HOMO of the chloroiron complex of TPCorr is somewhat lower. While the similarity of the calculated energies of the HOMOs of the two OECorr complexes cannot be considered quantitatively, and there is a difference in the identity of the HOMO found for the two complexes, the calculated energy difference is qualitatively consistent with the relatively small difference in the electrochemical potential for 1-electron oxidation of these two complexes in methylene chloride (0.43 and 0.76 V vs. SCE, respectively),[6] and suggests that the potential for 1-electron oxidation of [FeCl(TPCorr)] should be more positive than that for [FeCl(OECorr)], as is observed (1.07 V vs. SCE in methylene chloride).[9] This apparent correlation also suggests that electrochemical potentials cannot reliably define the *site* of oxidation or reduction (metal vs. corrolate ligand), and that, in fact, such a concept is, in at least some cases, meaningless. In contrast, this work suggests that (i) iron corrolates are extremely covalent complexes whose electron configurations cannot be readily defined from any one type of experimental data, (ii) that calculations of orbital energies and spin densities are required in order to achieve an understanding of these systems, (iii) that iron corrolates can have both extensive α and β spin density on the macrocycle, *whether or not* these spin densities cancel, and (iv) that the highly covalent, yet spin segregated, nature of these iron corrolates is indicative of a possible "oxidation state buffer" role for these complexes that may uniquely position the corrolate ligand to aid in the reactivity of these complexes as oxidation catalysts related to the cytochromes P450. Suffice it to say that the statement that the corrolate macrocycle is capable of stabilizing higher oxidation states of metals than is the porphyrinate macrocycle[1] is, as we now know, at best misleading, and it totally misses the incredible uniqueness of the corrolate macrocycle that we have found in this work. It seems likely that similar multiple-technique investigations of other metal corrolates, including those of Mn and MnCl (which have been proposed to have oxidation states ranging from II to IV),[9,42] Co(III),[9] and SnCl(IV),[8] will uncover at least some similar cases of difficulty in defining electron configurations, and at least some similar cases of the existence of significant α and β spin density on the macrocycle.

Acknowledgment. The support of the Deutsche Forschungsgemeinschaft, grant Tr97/31-1 (A.X.T.), the U.S. NationalInstitutes of Health, grant DK31038 (F.A.W.), NATO grant CRG971495 (S.L.), and MURST (S.L.) is gratefully acknowledged. The authors also wish to thank Ms. Cadia D'Ottavi for her valuable technical assistance in the synthesis of the complexes.

Supporting Information Available: Additional Mössbauer spectra, NMR Curie plot, electron and spin density plots obtained from DFT calculations (PDF). This material is available free of charge via the Internet at http://pubs.acs.org.

JA012701H